Absolute electron-impact-ionization cross-section measurements of the halogen atoms

Todd R. Hayes, Robert C. Wetzel, and Robert S. Freund

AT&T Bell Laboratories, Murray Hill, New Jersey 07974

(Received 23 July 1986)

Electron-impact-ionization cross sections have been measured for the halogen atoms F, Cl, Br, and I from threshold to 200 eV. The absolute accuracy is $\pm 14\%$, except for F which is $\pm 20\%$. The halogen cross sections have shapes similar to those of the neighboring rare gases but are greater in magnitude. Simple semiclassical formulas of electron-impact ionization are able to accurately predict the experimentally determined halogen to rare gas cross-section ratios.

I. INTRODUCTION

Accurate absolute cross sections for ionization of atoms and molecules by electron impact are required in many fields such as mass spectrometry, astrophysics, fusion technology, gas discharges, and modeling of semiconductor processing. Measured cross sections are available for only about two dozen atoms, however, and methods of calculating or estimating unmeasured cross sections are insufficiently accurate for many other atoms. We report here the first measurements of the cross sections for ionization of the halogen atoms F, Cl, Br, and I by electron impact.

The halogen atoms are of particular importance in plasma processing technologies used by the microelectronics industry for etching of semiconductors and metals. The availability of cross sections for the halogen atoms also provides the opportunity for direct comparisons with those of the rare gases, the neighboring group of the Periodic Table. Such comparisons should help us refine our ability to estimate unmeasured cross sections for other atoms.

II. EXPERIMENTAL SECTION

The companion paper[1] describes in detail the experimental apparatus, calculational procedures, and error analysis of these measurements of absolute ionization cross sections. Briefly, a fast-neutral-atom beam is prepared by charge-transfer neutralization of a mass-selected halogen atomic ion beam (3 keV). The atom beam then crosses a 0—200-eV electron beam of known flux and spatial profile. The products of electron-impact ionization are focused on the entrance to a hemispherical energy analyzer. The analyzer serves to separate ions of differing charge states. The flux of the neutral beam is monitored by a secondary electron detector, which is calibrated with a pyroelectric detector. The accuracy of measurements made with this experimental apparatus has been assessed to be approximately $\pm 15\%$ by evaluating the systematic and random error. The reliability of this estimate has been verified[1] by measuring the absolute ionization cross sections of the rare gases; we find agreement with those previous measurements which are generally accepted to be the most accurate available.[2-4]

Table I lists the source compounds and charge-transfer gases which were used to produce neutral-atom beams from positive- and negative-ion beams. Halogen ions were produced in the source region either by a dc discharge through a halogenated gas or by vaporization and ionization of group IA or IIA halide salts within a rare-gas dc discharge. The salts were contained within a stainless-steel charge holder which was heated by radiation from the source filament. Either positive or negative ions were extracted from the source region by appropriate voltage biasing. Positive ions were neutralized by charge transfer with a gas chosen to have a filled orbital resonant with the ion ground state. Gases for collisional detachment of negative ions were empirically selected to optimize the signal to background ratio. Pressures in the charge-transfer chamber ranged from 0.1 to 1.0 mTorr.

Although the solid sources (halide salts) generally gave

TABLE I. Production of halogen atom beams.

Ion	Production of halogen ions	Gas used for charge-transfer neutralization (or collisional detachment) of ions
F^-	SiF_4 discharge	1,3-butadiene
Cl^+	CCl_4 discharge; CF_2Cl_2 discharge; NaCl in a Kr discharge	ethane or 1,3-butadiene
Br^+	CF_2Br_2 discharge	ethane
I^+	NaI in a Ne or Kr discharge	ethane

TABLE II. Measured cross sections and multiple-ion ratios.

Atom	Energy (eV)	Single-ionization cross section ($\mathrm{\AA}^2$)	Energy (eV)	Multiple-ion ratios ($\times 100$) $100I(X^{2+})/I(X^+)$	$100I(X^{3+})/I(X^+)$
F	100	0.98 ± 0.17[a]			
Cl	70	3.47 ± 0.30			
Br	70	4.32 ± 0.12	150	8.47 ± 0.38	0.77 ± 0.04
I	100	5.55 ± 0.26	150	11.7 ± 0.5	4.0 ± 0.3

[a]The uncertainties are statistical, only.

the most intense beams of halogen cations, they were also found to yield hydrogen halides, HX^+, to varying degrees. The degree of contamination of the beam by HX was found to correlate with the hygroscopicity of the material. For example, $CaCl_2$ in a rare-gas discharge produced significant quantities of HCl (up to 50% of the beam content), while NaCl yielded no measurable HCl. NaF was found to yield both HF and F. Due to inadequate resolution at higher mass, the ion source velocity filter was capable of resolving HX^+ from X^+ only in the cases of F and Cl. Threshold studies could distinguish only between HF and F, since this is the only pair with sufficiently separated ionization potentials ($\Delta E_I = 1.44$ eV).

The F and Cl absolute cross sections given herein were obtained using beams which were free of HX contamination. The Br data were acquired using the liquid source CF_2Br_2 (which is expected to be free of HBr). The I data, however, were acquired using NaI, which is hygroscopic. We were unable to determine if or to what extent the beam was contaminated with HI. However, we found that with Cl beams the measured cross section was statistically invariant whether or not the beam was contaminated with varying amounts of HCl (operating so as not to resolve HCl from Cl at the velocity filter). This suggests that the ionization cross section of Cl is nearly the same as the sum of the cross sections for producing HCl^+ and Cl^+ from HCl (we are unable to resolve HCl^+ and Cl^+ in the final mass selection step). We expect that the I system should behave similarly, such that the measured cross section for I should not be significantly perturbed by small amounts of HI in the beam.

The energy scales were determined by linear regression analysis of the single-ionization cross section in the near-threshold region, assigning the intercept to the spectroscopic ionization potential of the ground-state atom.[5] For F and Cl, the fine-structure splitting in the atom and ion ground states is negligible (0.13 eV or less[6]). For Br and I the fine structure[6] is comparable to the 0.7 eV full width at half maximum (FWHM) energy spread of the electron beam, but we ignore its effect since no structure is observed. The same energy scale was used for the multiple-ion cross sections. Experimental ionization energies of the multiple ions were determined from fits of $\sigma^{1/n}$ versus E, where n is the charge on the ion. This procedure linearizes the threshold regions[7] such that an intercept may more readily be determined. While there is some ambiguity in the actual intercept because of poor signal-to-noise

ratio and an uncertain baseline, all ionization energies determined in this fashion agreed to within 2 eV of the spectroscopic ionization energies.[6]

III. RESULTS

Measurements of the absolute single-ionization cross sections for the process $X + e^- \rightarrow X^+ + 2e^-$ were made at electron energies near the peak of the cross section versus energy curve for each halogen atom. Table II lists mean cross-section values and statistical standard deviations for single ionization of each halogen atom, for the energy at which the measurements were most commonly made. Five measurements were made for Br and I, eight for Cl, and 11 for F. Also listed are the mean cross-section ratios which were used in scaling the double- and triple-ionization cross sections. Four or five measurements were made for each of the multiple-ion ratios. The relative intensities of multiply charged ions were determined by measuring the intensity ratios $I(X^{n+})/I(X^+)$. Cross sections for the production of the multiply charged ions were calculated using this ratio.

Ion signal versus electron energy was measured from threshold to 200 eV, and scaled to the absolute cross section determined at a single energy. For the fluorine and chlorine atoms, only the partial cross sections for single ionization could be measured; signal-to-noise levels were
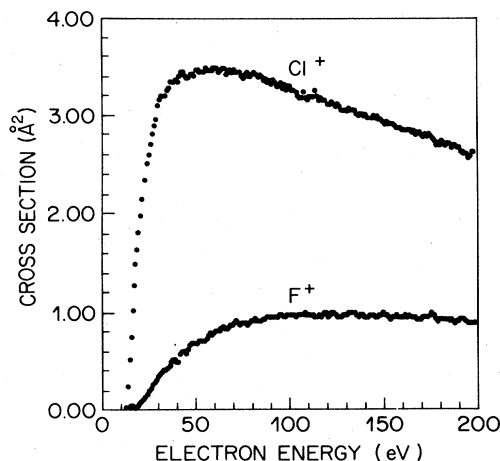

FIG. 1. Single-ionization cross sections for fluorine and chlorine from 0 to 200 eV.
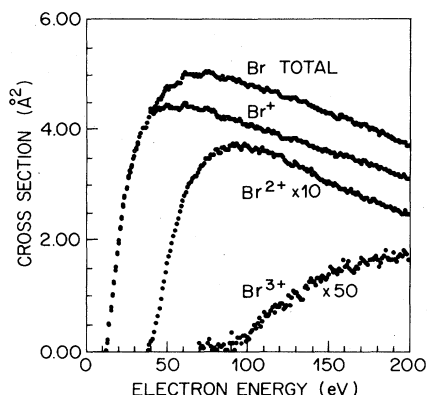
FIG. 2. Cross sections for single, double, and triple ionization of Br, and the total ionization cross section, from 0 to 200 eV.

very low for multiple-ionization processes. For the bromine and iodine atoms, partial ionization cross sections were measured from threshold to 200 eV for the processes $X+e^-\rightarrow X^{n+}+(n+1)e^-$ where $n=1$, 2, and 3. The charge-weighted partial cross sections at a given energy are added to give the total ionization cross section using the formula $\sigma_{total}=\sigma^++2\sigma^{2+}+3\sigma^{3+}$. The partial and total ionization cross sections for the four halogen atoms are given in Figs. 1—3, and in Tables III and IV. Absolute cross sections and ion ratios measured at a number of energies were compared to the ion signal versus electron energy curves to check the consistency of the method.

The experimental method was optimized for absolute cross section measurements in the 50 to 150 eV range. Effects such as electron reflection and electron-beam spreading lead to cross sections that are slightly low below 50 eV and slightly high above 150 eV. In the rare-gas study[1] a polynomial function was obtained which when applied to the cross section versus energy data minimizes systematic energy-dependent deviations and yields more accurate cross-section data. Both the raw data and the adjusted data are included here. The figures contain data adjusted
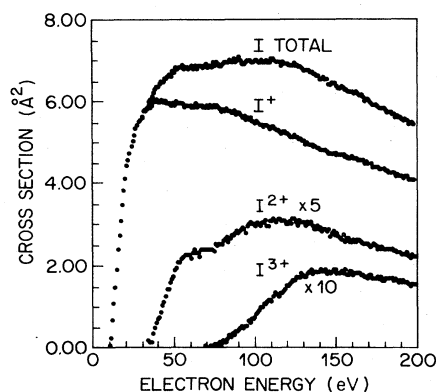

FIG. 3. Cross sections for single, double, and triple ionization of I, and the total ionization cross section, from 0 to 200 eV.

by applying the polynomial correction function. The tables contain both raw and adjusted data. We recommend use of the adjusted data, as we believe them to be slightly closer to the correct cross sections.

IV. DISCUSSION

A. Accuracy of measurements

In the fast beam experimental method employed here all parameters necessary for the absolute cross section determination are either directly measured or accurately estimated. A complete analysis of the accuracy of the method (given in the companion paper[1]) gives $\pm12\%$ for the systematic error. The statistical uncertainties are $\pm17\%$ for F, $\pm8.6\%$ for Cl, $\pm2.8\%$ for Br, and $\pm4.7\%$ for I. For the I atom measurements, an additional uncertainty is introduced by the possible presence of HI in the beam, but as discussed above, we do not expect the contaminant to have a significant effect on the measured cross section. The trends observed in comparisons of the halogen and rare-gas cross-section data (see the following) support the integrity of the I data. We conclude that the accuracy of the I data is equivalent to that of the other halogens. The total uncertainty of each absolute cross-section value is calculated by combining the systematic and statistical uncertainties in quadrature. The resulting uncertainties are $\pm20\%$ for F, $\pm14\%$ for Cl, $\pm11\%$ for Br, and $\pm12\%$ for I. The large uncertainty for F is primarily due to the large statistical spread in the data, a result of low signal-to-noise ratio in this measurement.

B. Halogen and rare-gas comparisons

Simple inspection reveals a striking similarity between each halogen ionization cross section and that of the neighboring rare gas (see companion paper[1]). The shapes are nearly identical and the halogen cross sections are slightly larger. This comparison is made quantitatively in Figs. 4 and 5, which show the cross-section ratios of each halogen and its neighboring rare gas. The energy scale for each atom is normalized to its ionization potential (before calculating the ratio) to enable a direct comparison of the shapes. In Fig. 4, the single ionization cross section ratios σ_X^+/σ_{RG}^+ for each halogen—rare-gas pair are plotted versus the reduced energy E/E_I. In Fig. 5, the double-ionization ratios $\sigma_X^{2+}/\sigma_{RG}^{2+}$ for Br and I are plotted versus energy divided by the experimental double-ionization potential. The two dominant features of these ratios are that they are greater than unity and are nearly constant over reduced energy. The systematic uncertainty in the ratio values is $\pm10\%$. (This is smaller than the absolute cross-section uncertainty because the electron reflection and detector efficiency terms cancel[1] in the ratio.) Variations near threshold are primarily due to low signal-to-noise ratio and small inaccuracies in the energy scales. The similarity of the shapes is not surprising when one considers the similarity of the electron configurations of the halogens and their rare-gas neighbors. The somewhat larger deviation from constancy for the $\sigma(F^+)/\sigma(Ne^+)$ ratio may represent a real difference in the shapes, but we cannot now offer an interpretation.

TABLE III. Cross section vs electron-energy data for single ionization of F, Cl, Br, and I.

Energy (eV)	Cross section (Å^2)							
	F^+		Cl^+		Br^+		I^+	
	raw	adj.	raw	adj.	raw	adj.	raw	adj.
10	0.00	0.00	0.00	0.00	0.00	0.00	0.04	0.04
11	0.00	0.00	0.00	0.00	0.00	0.00	0.23	0.25
12	0.00	0.00	0.01	0.01	0.04	0.04	0.60	0.65
13	0.00	0.00	0.02	0.02	0.21	0.22	1.00	1.08
14	0.00	0.00	0.23	0.24	0.50	0.54	1.39	1.49
15	0.04	0.04	0.48	0.52	0.76	0.81	1.79	1.92
16	0.04	0.05	0.69	0.74	0.98	1.04	2.23	2.38
17	0.02	0.03	0.95	1.01	1.20	1.27	2.58	2.75
18	0.02	0.03	1.19	1.27	1.43	1.52	2.90	3.08
19	0.05	0.06	1.41	1.50	1.68	1.79	3.30	3.50
20	0.06	0.07	1.55	1.65	1.89	2.00	3.60	3.82
21	0.08	0.09	1.71	1.81	2.11	2.23	3.92	4.15
22	0.11	0.12	1.88	1.99	2.31	2.44	4.19	4.43
23	0.13	0.14	2.05	2.16	2.53	2.67	4.35	4.59
24	0.15	0.16	2.22	2.34	2.69	2.83	4.50	4.74
25	0.18	0.19	2.38	2.50	2.84	2.98	4.68	4.92
26	0.21	0.22	2.47	2.59	3.01	3.16	4.82	5.05
27	0.24	0.26	2.58	2.71	3.11	3.26	4.93	5.17
28	0.27	0.29	2.67	2.80	3.21	3.36	5.10	5.34
29	0.28	0.30	2.77	2.89	3.36	3.51	5.20	5.43
30	0.33	0.34	2.84	2.96	3.47	3.62	5.30	5.53
32	0.38	0.39	3.03	3.16	3.63	3.78	5.41	5.63
34	0.40	0.41	3.08	3.20	3.81	3.96	5.56	5.78
36	0.44	0.46	3.16	3.27	3.91	4.05	5.73	5.93
38	0.50	0.52	3.24	3.35	4.01	4.14	5.76	5.94
40	0.47	0.48	3.25	3.35	4.21	4.34	5.85	6.03
45	0.59	0.61	3.35	3.43	4.26	4.37	5.86	6.01
50	0.67	0.68	3.37	3.44	4.35	4.43	5.84	5.96
55	0.71	0.72	3.42	3.47	4.33	4.40	5.87	5.97
60	0.77	0.78	3.45	3.49	4.38	4.43	5.86	5.93
65	0.82	0.83	3.46	3.49	4.38	4.42	5.86	5.91
70	0.87	0.87	3.45	3.47	4.34	4.36	5.87	5.91
75	0.88	0.88	3.43	3.44	4.36	4.37	5.88	5.90
80	0.90	0.90	3.43	3.43	4.30	4.31	5.84	5.85
85	0.92	0.92	3.43	3.43	4.23	4.23	5.81	5.80
90	0.96	0.95	3.37	3.37	4.22	4.22	5.75	5.74
95	0.96	0.96	3.35	3.34	4.17	4.16	5.65	5.63
100	0.98	0.98	3.32	3.31	4.12	4.10	5.57	5.55
105	0.97	0.97	3.25	3.23	4.09	4.06	5.50	5.47
110	0.98	0.98	3.22	3.20	4.02	3.99	5.44	5.41
115	0.97	0.96	3.23	3.21	4.00	3.97	5.38	5.34
120	0.99	0.98	3.18	3.15	3.92	3.89	5.30	5.26
125	0.99	0.98	3.15	3.13	3.88	3.85	5.21	5.16
130	0.99	0.98	3.10	3.07	3.86	3.83	5.13	5.08
135	0.99	0.98	3.09	3.05	3.83	3.79	5.03	4.98
140	0.97	0.96	3.05	3.01	3.75	3.71	4.95	4.89
145	0.98	0.97	3.02	2.97	3.71	3.65	4.88	4.81
150	0.99	0.98	3.00	2.96	3.67	3.61	4.82	4.74
155	0.97	0.95	2.96	2.91	3.62	3.55	4.77	4.69
160	0.98	0.96	2.91	2.85	3.62	3.55	4.74	4.64
165	0.98	0.96	2.91	2.84	3.57	3.49	4.70	4.59
170	0.97	0.94	2.89	2.81	3.53	3.44	4.64	4.52
175	0.99	0.96	2.87	2.78	3.50	3.40	4.55	4.42
180	0.96	0.92	2.82	2.72	3.44	3.32	4.51	4.35
185	0.97	0.93	2.82	2.71	3.43	3.29	4.45	4.28
190	0.96	0.92	2.81	2.68	3.36	3.21	4.40	4.21
195	0.95	0.91	2.75	2.61	3.35	3.18	4.36	4.14
200	0.95	0.90	2.79	2.63	3.34	3.14	4.32	4.07

TABLE IV. Cross section vs electron-energy data for double and triple ionization of Br and I.

Energy (eV)	Br^{2+} raw	Br^{2+} adj.	Br^{3+} raw	Br^{3+} adj.	I^{2+} raw	I^{2+} adj.	I^{3+} raw	I^{3+} adj.
30	0.000	0.000			0.002	0.002		
32	0.000	0.000			0.005	0.005		
34	0.001	0.001			0.037	0.038		
36	0.001	0.001			0.031	0.032		
38	0.005	0.005			0.098	0.101		
40	0.018	0.019			0.141	0.145		
45	0.079	0.081			0.249	0.255		
50	0.153	0.156			0.352	0.359		
55	0.214	0.218			0.426	0.433		
60	0.268	0.272			0.446	0.451		
65	0.305	0.308			0.463	0.467		
70	0.327	0.329	0.0035	0.0015	0.476	0.479	0.003	0.003
75	0.347	0.348	0.0023	0.0023	0.484	0.485	0.008	0.008
80	0.360	0.360	0.0013	0.0013	0.514	0.514	0.015	0.015
85	0.366	0.366	0.0017	0.0017	0.538	0.538	0.030	0.030
90	0.372	0.371	0.0030	0.0030	0.566	0.565	0.046	0.046
95	0.372	0.371	0.0046	0.0046	0.586	0.584	0.057	0.057
100	0.371	0.370	0.0054	0.0054	0.607	0.604	0.077	0.077
105	0.366	0.364	0.0099	0.0099	0.610	0.607	0.104	0.103
110	0.365	0.362	0.0123	0.0122	0.616	0.612	0.120	0.119
115	0.360	0.357	0.0154	0.0153	0.629	0.624	0.134	0.133
120	0.357	0.354	0.0168	0.0167	0.617	0.612	0.151	0.149
125	0.344	0.341	0.0181	0.0180	0.617	0.612	0.170	0.168
130	0.341	0.337	0.0210	0.0208	0.615	0.609	0.179	0.177
135	0.334	0.331	0.0218	0.0215	0.605	0.598	0.190	0.188
140	0.328	0.324	0.0257	0.0254	0.587	0.580	0.191	0.189
145	0.317	0.312	0.0268	0.0264	0.576	0.568	0.190	0.187
150	0.310	0.305	0.0284	0.0280	0.563	0.554	0.191	0.188
155	0.304	0.299	0.0293	0.0287	0.540	0.531	0.189	0.185
160	0.299	0.293	0.0319	0.0312	0.533	0.522	0.188	0.184
165	0.297	0.290	0.0304	0.0297	0.529	0.517	0.186	0.182
170	0.289	0.282	0.0331	0.0323	0.515	0.502	0.181	0.176
175	0.283	0.274	0.0334	0.0325	0.509	0.494	0.177	0.172
180	0.281	0.271	0.0339	0.0327	0.501	0.483	0.175	0.169
185	0.274	0.263	0.0354	0.0340	0.495	0.476	0.176	0.169
190	0.270	0.258	0.0352	0.0336	0.480	0.459	0.173	0.165
195	0.266	0.252	0.0370	0.0351	0.476	0.452	0.167	0.159
200	0.264	0.249	0.0321	0.0302	0.474	0.447	0.166	0.156

Good agreement is found between the halogen to rare-gas ratios and the ratios predicted by semiclassical and semiempirical approximations of electron-impact ionization. These are simple models that address both the scaling of the ionization cross section with atomic number, and the shape of the cross section versus energy curve.[8] Most of the formulas are modifications of that of Thomson,[9] which employs the Rutherford formula for the scattering of two free electrons in describing single ionization. Ionization from each orbital is considered separately. Most of the formulas have the form

$$\sigma_n = kq_n P_n^{-2} g(u) \; .$$

Here σ_n is the cross section for ionization from orbital n, k is a scaling constant, q_n is the orbital occupation number, and P_n is the orbital energy. The function $g(u)$, where $u = E/P_n$, gives the shape of the cross section with

energy. The ionization cross section σ^+ is the sum of the contributions of all the orbitals in the atom, i.e., $\sigma^+ = \sum_n \sigma_n$.

Experimentally, the halogen to rare-gas ratios are nearly constant over E/E_I, and so the $g(u)$ term which gives the cross section its shape is neglected in the ratio calculation. The resulting ratio expression:

$$\frac{\sigma_X^+}{\sigma_{RG}^+} = \frac{\sum_n (q_n P_n^{-2})_X}{\sum_n (q_n P_n^{-2})_{RG}}$$

has been used to calculate the cross-section ratios for neighboring atoms. Only electrons in the s and p valence shells have been included; the contributions of core electrons to the sums are found to be negligible. The results in Table V, column 4 agree well with the measured ratios

of the peak cross sections given in column 2. If the con-
tributions of the s orbitals are neglected, and only the p
electrons are used in the calculation, the ratios are still
within 2% of those given in Table V. We conclude that
the $q_n P_n^{-2}$ term found in most of the semiempirical and

TABLE V. Comparison of experimental and theoretical
single-ionization cross-section ratios.

Atom	Ratio at peak (exp)	$100\sum_n q_n P_n^{-2}$ [a]	Ratio (calc)
F	1.34	1.79	1.30
Ne		1.38	
Cl	1.29	3.30	1.25
Ar		2.65	
Br	1.18	3.93	1.17
Kr		3.35	
I	1.18	5.12	1.14
Xe		4.50	

[a]Using s and p valence orbitals.

semiclassical approximations is able to predict the mea-
sured halogen to rare-gas single-ionization ratios.

Although most of the cross-section curves in Figs. 1—3
are fairly featureless, the I^+ and I^{2+} curves exhibit two
peaks. Very similar structure is observed for Xe^+ and
Xe^{2+} curves. This structure has been discussed for Xe
(Ref. 10) and is poorly understood. It appears that it can-
not be fully explained by $4d$ excitation-autoionization pro-
cesses. It is conceivable that the oscillation in the
$\sigma(I^{2+})/\sigma(Xe^{2+})$ ratio (Fig. 5) results from this structure.
We cannot, however, rule out the possibility that this os-
cillation may be in part due to HI contamination in the I
beam.

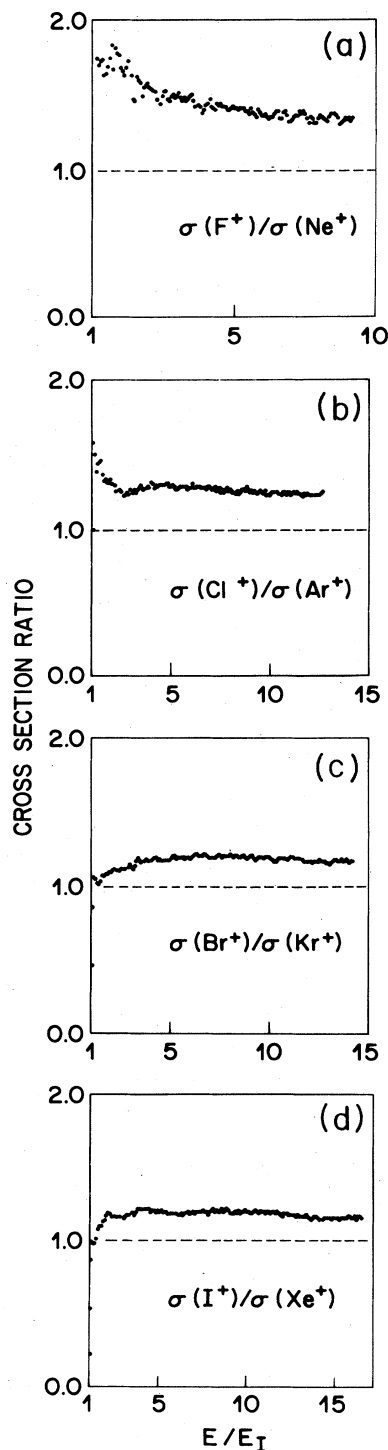FIG. 4. Single-ionization cross-section ratios vs E/E_I. (a)
$\sigma(F^+)/\sigma(Ne^+)$, (b) $\sigma(Cl^+)/\sigma(Ar^+)$, (c) $\sigma(Br^+)/\sigma(Kr^+)$, (d)
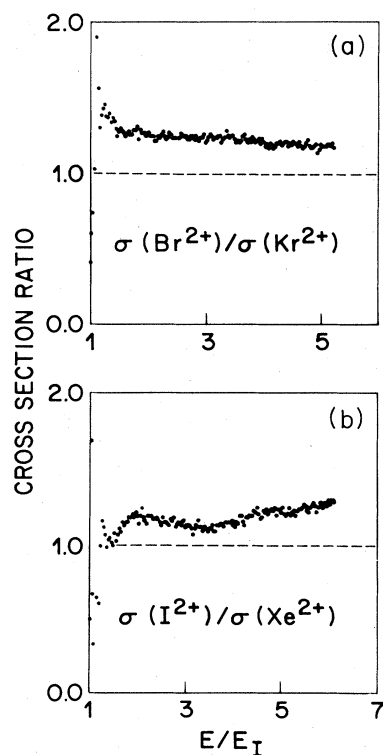$\sigma(I^+)/\sigma(Xe^+)$.

FIG. 5. Double-ionization cross-section ratios vs E/E_I. (a)
$\sigma(Br^{2+})/\sigma(Kr^{2+})$, (b) $\sigma(I^{2+})/\sigma(Xe^{2+})$.

V. SUMMARY

Absolute electron-impact ionization cross sections for the halogen atoms have been measured for the first time. Partial cross sections for single ionization of F, Cl, Br, and I are reported for the energy range from threshold to 200 eV. Partial cross sections for ionization to doubly and triply charged ions have also been measured for Br and I. The total ionization cross sections for Br and I have been calculated from the charge-weighted sums of the partial cross sections.

The shapes of the halogen cross sections are found to be markedly similar to those of the neighboring rare-gas atoms. The magnitudes for the halogens are found to be slightly larger than those of the neighboring rare gases, ranging from about 30% larger for the F and Ne ratio to about 14% larger for the I to Xe ratio. Ratios predicted by semiclassical approximations agree well with the observations, strengthening our confidence in the utility of these simple approaches for correlating or predicting other cross sections.

---

[1]R. C. Wetzel, F. A. Baiocchi, T. R. Hayes, and R. S. Freund, preceeding paper, Phys. Rev. A **xx**, xxxx (1986).

[2]R. G. Montague, M. F. A. Harrison, and A. C. H. Smith, J. Phys. B **17**, 3295 (1984).

[3]D. Rapp and P. Englander-Golden, J. Chem. Phys. **43**, 1464 (1965).

[4](a) K. Stephan, H. Helm, and T. D. Märk, J. Chem. Phys. **73**, 3763 (1980). (b) K. Stephan and T. D. Märk, J. Chem. Phys. **81**, 3116 (1984).

[5]R. D. Levin and S. G. Lias, *Ionization and Appearance Potential Measurements, 1971—1981*, Natl. Bur. Stand. Ref. Data Ser., Natl. Bur. Stand. (U.S.) Circ. No. 71 (U.S. GPO, Washington, D.C., 1982). Ionization potentials (eV): $E_I(F) = 17.42$, $E_I(Cl) = 12.97$, $E_I(Br) = 11.81$, $E_I(I) = 10.43$, for the $(^2P^o_{3/2} \rightarrow {}^3P_2)$ transition.

[6]C. E. Moore, *Ionization Potentials and Ionization Limits Derived from the Analyses of Optical Spectra*, Natl. Bur. Stand. Ref. Data Ser., Natl. Bur. Stand. (U.S.) Circ. No. 34 (U.S. GPO, Washington, D.C., 1970).

[7]F. H. Read, in *Electron Impact Ionization*, edited by T. D. Märk and G. H. Dunn (Springer-Verlag, New York, 1985), p. 58.

[8]S. M. Younger and T. D. Märk, in *Electron Impact Ionization*, edited by T. D. Märk and G. H. Dunn (Springer-Verlag, New York, 1985), Chap. 2.

[9]J. J. Thomson, Philos. Mag. **23**, 449 (1912).

[10]D. Mathur and C. Badrinathan, *Abstracts of the 14th International Conference on the Physics of Electronic and Atomic Collisions, Palo Alto, 1985*, edited by M. J. Coggiola, D. L. Hoestis, and R. P. Saxon (ICPEAC, Palo Alto, 1985), p. 167.